

# Interpolation and Averaging of Multi-Compartment Model Images

Renaud Hédouin<sup>1</sup>, Olivier Commowick<sup>1</sup>, Aymeric Stamm<sup>2</sup>,  
and Christian Barillot<sup>1</sup>

<sup>1</sup> VISAGES: INSERM U746, CNRS UMR6074, INRIA, Univ. of Rennes I, France

<sup>2</sup> CRL, Children's Hospital Boston, Harvard Medical School, Boston, USA

**Abstract.** Multi-compartment diffusion models (MCM) are increasingly used to characterize the brain white matter microstructure from diffusion MRI. We address the problem of interpolation and averaging of MCM images as a simplification problem based on spectral clustering. As a core part of the framework, we propose novel solutions for the averaging of MCM compartments. Evaluation is performed both on synthetic and clinical data, demonstrating better performance for the “covariance analytic” averaging method. We then present an MCM template of normal controls constructed using the proposed interpolation.

## 1 Introduction

Diffusion Weighted Imaging (DWI) is a unique MRI acquisition strategy, which can provide invaluable insights into the white matter architecture in-vivo and non-invasively. A number of diffusion models have been devised, with the aim to characterize the underlying tissue microstructure. The most widespread model is known as Diffusion Tensor Imaging (DTI) [3] which, under the assumption of homogeneous diffusion in each voxel, describes the random motion of water as a single Gaussian process with a diffusion tensor. However, many regions of crossing fibers exist in low-resolution clinical DWI and the DTI model fails at correctly representing them. Multi-compartment models (MCM) have been extensively proposed and studied as alternative diffusion models to cope with the intrinsic voxelwise diffusion heterogeneity [4]. The key principle of MCM is to explicitly model the diffusion in a number of pre-specified compartments akin to groups of cells inducing similar diffusion properties. MCMs may have a great impact on patient care, as they allow for a better characterization of brain tissue microstructure, which enables the identification of more specific biomarkers such as proportion of free water (edema), proportion of water in axons (partial disruption or complete loss of axons, axonal injury), etc.

A critical step to identify relevant biomarkers on a large database is the creation of an atlas from individual estimated MCM images. This is achieved using registration and interpolation of MCMs. To date, only few approaches have addressed this issue. Among them, Barmpoutis et al. [2] or Geng et al. [5] introduced registration methods specifically tuned for Orientation Distribution Functions (ODF) on the sphere. Goh et al. [6] introduced an interpolation method

for ODFs in a spherical harmonics basis as a Riemannian average. However, this approach does not apply to MCMs as they are not expressed in the same basis. Taquet et al. [13] proposed an interpolation approach seen as a simplification problem of all weighted compartments from a set of voxels into a smaller set of compartments. However, they assume that a single compartment belongs to the exponential family which is not the case for all MCMs.

We introduce a new interpolation method for MCM images also as a simplification problem. It relies on the fuzzy spectral clustering [9] of input compartments, from MCMs provided e.g. from trilinear interpolation, into a predefined number of output compartments. Then, each cluster is used to compute an interpolated compartment, providing an output MCM. This method is very generic as it relies only on the definition of a similarity measure between compartments and of a weighted averaging scheme for compartments. It can therefore be applied to any MCM as long as those two components may be defined.

In the following, we present MCM interpolation / averaging as a simplification problem based on spectral clustering (Section 2.1). Then, we define 4 possible compartment averaging methods for the Diffusion Directions Imaging (DDI) model [11] in Section 3 and similarity measures related to each of those averaging schemes. We demonstrate qualitatively and quantitatively the interest of both the averaging schemes and interpolation framework on simulated and in vivo data. We finally apply this framework to compute an atlas of DDI (Section 3) which clearly highlights average crossing fiber regions.

## 2 Theory

### 2.1 Model Interpolation as a Simplification Problem

We consider  $m$  MCM  $M^i (i = 1, \dots, m)$  each containing  $c(i)$  compartments of constrained water diffusion and a free water compartment describing isotropic unconstrained water diffusion. We note  $F_j^i$  the  $j$ -th compartment of  $M^i$  and  $F_{\text{free}}^i$  its free water compartment, their respective weights being  $w_j^i$  and  $w_{\text{free}}^i$  and sum to 1. Each of these  $M^i$  has an associated weight  $\alpha^i$ . For example, in the case of a trilinear interpolation, we have 8 MCM with spatial weights  $\alpha^i$ . We formulate the interpolation problem as merging the  $M^i$  into one MCM with a predetermined number of compartments  $q$  and one free water compartment. There are therefore two different averaging parts: compartments and free water compartment.

The averaging of all compartments coming from  $M^i$  into  $q$  compartments is performed using spectral clustering [9]. Having defined a similarity matrix  $S$  between compartments, spectral vectors are extracted from  $S$ . These spectral vectors are then clustered using fuzzy C-Means. Hence, we obtain  $q$  sets of  $n$  weights ( $n$  being the total number of compartments)  $\beta_{j,k}^i$  that are probabilities for the  $j$ -th compartment of  $M^i$  to belong to the  $k$ -th cluster. We define  $\theta_{j,k}^i$  the

weight of the  $j$ -th compartment of  $M^i$  in the  $k$ -th cluster and  $\theta_i$  the weight of the free water compartment of  $M^i$ :

$$\theta_{j,k}^i = \alpha^i w_j^i \beta_{j,k}^i, \quad \theta_i = \alpha^i w_{\text{free}}^i \quad (1)$$

From  $\theta_{j,k}^i$  and  $\theta_i$ , we compute weights  $\phi_k$  and  $\phi_{\text{free}}$  of the output compartments.

$$\forall k = 1, \dots, q \quad \phi_k = \sum_{i=1}^m \sum_{j=1}^{c(i)} \theta_{j,k}^i, \quad \phi_{\text{free}} = \sum_{i=1}^m \theta_i \quad (2)$$

We also define  $\hat{\theta}_{j,k}^i$  and  $\hat{\theta}_i$  two different sets of normalized weights from  $\theta_{j,k}^i$  and  $\theta_i$ . This framework is very generic and can be applied to any MCM as long as we provide a way to compute a similarity matrix between compartments. Free water averaging is common to any MCM and is described in Section 2.2. We derive MCM compartments averaging for DDI in Section 2.3 and similarity matrix computation in Section 2.4.

## 2.2 Free Water Compartments Averaging

We estimate from the isotropic diffusivities  $d_{\text{free}}^i$  of  $M^i$  the diffusivity  $d_{\text{free}}$  of the average model associated to weight  $\phi_{\text{free}}$ . Free diffusion follows an isotropic Gaussian distribution with covariance matrix  $D_{\text{free}}^i = d_{\text{free}}^i I_3$  (where  $I_3$  is the identity matrix). The averaging is performed using the log-Euclidean framework [1]:

$$D_{\text{free}} = \exp\left(\sum_{i=1}^m \hat{\theta}_i \log(D_{\text{free}}^i)\right) \Rightarrow d_{\text{free}} = \exp\left(\sum_{i=1}^m \hat{\theta}_i \log(d_{\text{free}}^i)\right) \quad (3)$$

## 2.3 MCM Compartments Averaging

We propose four different methods to average DDI compartments into a single one: classic, tensor, log VMF, and covariance analytic. For each cluster  $k$ , we wish to average the set of  $F_j^i$  with weights  $\hat{\theta}_{j,k}^i$  into a compartment  $C_k$  with weight  $\phi_k$ . To simplify notations, we now just consider  $n$  compartments  $F_i (i = 1, \dots, n)$  with their corresponding weights  $w_i$ .

### 2.3.1 Specification of the DDI Model

Each MCM has specific parameters and models for compartments. The compartment averaging part therefore cannot be exactly similar for any MCM. We choose to detail several compartments averaging methods for one particular MCM: the DDI model.

In addition to the free water compartment, a number of axonal compartments can be added to DDI to model how water molecules diffuse in axonal bundles with various orientations. Diffusing water molecules in a particular axonal compartment are assumed to undergo a random displacement that is the independent sum of a von Mises & Fisher (VMF) vector on  $S^2$  of radius  $r$  and a

Gaussian vector on  $\mathbb{R}^3$ . Hence, the resulting diffusion probability density function describing this random displacement is given by the 3D convolution of the VMF distribution with the Gaussian distribution:

$$p_{\mu,\kappa,d,\nu} = \text{Convolution}(\text{VMF}(\mu, \kappa, r), \text{Gaussian}(0, \frac{(1-\nu)d}{\kappa+1}[I_3 + \kappa\mu\mu^T])) \quad (4)$$

where  $\mu \in S^2$  is the principal axis of diffusion,  $\kappa$  an index of the concentration of diffusion around  $\mu$ ,  $d$  the diffusivity along  $\mu$ ,  $\nu$  the proportion of extra-axonal space in the compartment,  $r$  the radius of the VMF sphere given by  $r = \sqrt{\nu d}$ .  $\Sigma$  is the covariance matrix of the Gaussian part. Let  $\mu_i, \kappa_i, \nu_i, d_i$  be the parameters of  $F_i$  and  $\mu, \kappa, \nu, d$  be the parameters of the average compartment  $F$ .

**2.3.2 Common Part of Compartment Averaging**

We choose to average the sphere of radius  $r$  as the one whose surface is the average of the input sphere surfaces. This corresponds to a Euclidean average of the individual  $r_i^2$ :  $r^2 = \sum_{i=1}^n w_i r_i^2$ . This also gives us a direct relation between  $\nu$  and  $d$  leading to only 3 parameters to estimate ( $\mu, \kappa$  and  $\nu$ ),  $d$  being computed as  $d = r^2/\nu$ .

**2.3.3 Simple Averaging**

The simplest approach performs a weighted Euclidean averaging on each parameter except  $\mu$ . Each  $\mu_i$  is a direction in  $S^2$ . However, for the DDI model, they do not represent a direction but an orientation. The simplest way to solve this problem (as two opposite directions) is to put all  $\mu_i$  in the top hemisphere and average them on the sphere to obtain  $\mu$ .

**2.3.4 Tensor Averaging**

The simple averaging is however only a partial solution, especially for directions close to the sphere equator. We now consider  $\mu_i$  as orientations instead of directions.  $\mu_i$  is represented as a cigar-shaped tensor  $T_i \in \mathcal{S}_3^+(\mathbb{R})$  defined as:

$$T_i = \mu_i \mu_i^T + \varepsilon I_3 \quad (5)$$

With  $\varepsilon$  small to have non degenerated tensors. Then, we can average  $T_i$  using the log-Euclidean framework similarly to Eq. (3). We define the average  $\mu$  as the principal direction of  $T$  (eigenvector with the largest eigenvalue). The other parameters are obtained as for simple averaging.

**2.3.5 Covariance Analytic**

Another approach uses information from covariance matrices  $\Sigma_i$  of DDI compartments. These  $\Sigma_i$  matrices belong to  $\mathcal{S}_3^+(\mathbb{R})$  and can be averaged into  $\Sigma$  similarly to Eq. (3). We wish to extract all parameters from the average  $\Sigma$ . We start by approximating  $\Sigma$  by a cigar-shaped tensor to match the DDI compartment model. To do that, we need to enforce two equal secondary eigenvalues  $\lambda_{\perp}$ . In the log-Euclidean framework, this amounts to compute  $\lambda_{\perp}$  as  $\lambda_{\perp} = \sqrt{\lambda_2 \lambda_3}$  where  $\lambda_2, \lambda_3$  are the two lowest eigenvalues of  $\Sigma$ . We now have  $\hat{\Sigma}$  the cigar-shaped tensor of  $F$ :

$$\hat{\Sigma} = \frac{(1-\nu)d}{\kappa+1}[I_3 + \kappa\mu\mu^T] \quad (6)$$

Proceeding by identification and given that  $r^2 = \nu d$ , we obtain that  $\mu$  is the principal eigenvector of  $\hat{\Sigma}$ .  $\nu$  and  $\kappa$  are given by:

$$\nu = \frac{r^2}{\lambda + r^2}, \quad \kappa = 2 \frac{\lambda - \lambda_{\perp}}{\lambda_{\perp}} \tag{7}$$

### 2.3.6 Log VMF

We now explore the option to use the VMF to compute  $\mu$  and  $\kappa$  and recover only  $\nu$  from  $\hat{\Sigma}$ . We consider a VMF distribution as a point in a Riemannian manifold, similarly to the approach presented by McGraw et al. [8]. To interpolate several points, a geodesic on these manifolds is defined (refer to [8] for details). Orientation averaging is similar to tensor averaging as in Section 2.3.4. The interpolation of  $\kappa$  is done recursively by projection as in McGraw et al. Letting  $\kappa = \kappa_1$ , repeat until convergence (i.e until  $l_{\kappa} < \varepsilon$ ):

$$l_{\kappa} = \sum_{i=1}^n w_i \log\left(\frac{\kappa_i}{\kappa}\right) \tag{8}$$

$$\kappa = \kappa \exp(l_{\kappa}) \tag{9}$$

Knowing all parameters except  $\nu$ , we obtain it from  $\hat{\Sigma}$  as:

$$\nu = \frac{r^2[2r^2 + \lambda + \lambda_{\perp}(1 + \kappa)]}{2(r^2 + \lambda)[r^2 + \lambda_{\perp}(1 + \kappa)]} \tag{10}$$

## 2.4 Similarity Measure between Compartments

To perform spectral clustering, we need a similarity measure between compartments. To stay coherent with the compartment averaging part, they are defined following metrics associated with each method. In each case except covariance analytic, we compute separately the distance between  $\mu$ ,  $\kappa$ ,  $r$  and add them with normalization terms  $\alpha, \beta$  to give each parameters the same influence. For two compartments  $F_1$  and  $F_2$ , the similarity measures are defined as follows:

$$\left\{ \begin{array}{l} d_{\text{simple}}(F_1, F_2) = \langle \mu_1, \mu_2 \rangle^2 + \alpha|\kappa_1 - \kappa_2| + \beta|r_1 - r_2| \\ d_{\text{tensor}}(F_1, F_2) = \|\log(T_1) - \log(T_2)\| + \alpha|\kappa_1 - \kappa_2| + \beta|r_1 - r_2| \\ d_{\text{logVMF}}(F_1, F_2) = \|\log(T_1) - \log(T_2)\| + \alpha|\log(\kappa_1) - \log(\kappa_2)| + \beta|r_1 - r_2| \\ d_{\text{covariance analytic}}(F_1, F_2) = \|\log(\Sigma_1) - \log(\Sigma_2)\| \end{array} \right. \tag{11}$$

## 3 Experiments and Results

### 3.1 Compartment Averaging Evaluation on Simulated Data

We first evaluate compartment averaging into a single one. To do so, we simulate random DDI compartments by drawing parameter values from uniform distribution between different bounds depending on the parameter: 0 and 20 for  $\kappa$ ,

$5.10^{-4}m.s^{-2}$  and  $5.10^{-3}m.s^{-2}$  for  $d$ , 0 and 1 for  $\nu$ , and random orientation on  $S^2$  for  $\mu$ . Four random DDI compartments are computed, they correspond to the four corners of a grid of size  $11 \times 11$  that we want to extrapolate. To perform a robust experiment, we created a database of 500 sets of 4 corners. The reference is a grid containing 4 compartments per pixel with a weight proportional to the position of the voxel with respect to each corner (see Fig. 1.e). For each method, we average each pixel of the reference image into only one DDI compartment. To quantitatively evaluate DDI averaging, we simulate, for each method and the reference, a DWI signal from DDI models following Eq. (6) in [11] on 60 directions for each of 3 different b-values. A Euclidean distance between simulated DWIs of the 4 methods and the reference provides quantitative results.

The Euclidean distances on the 500 random images are normalized so that the simple error mean is 100. The result for the different methods are: simple: 100, tensor: 31.6, log VMF: 28.0, covariance analytic: 11.1. We present in Fig. 1 representative images from averaged DDI models superimposed on the corresponding error maps. The simple method has a large error explained by direction averaging. The tensor method is better: thanks to the orientation averaging part. However, there are still large errors which can be explained by large  $\kappa$  values in regions averaging orthogonal directions, which is not realistic. log VMF suffers from the same problem as tensor. Covariance analytic performs much better than all other methods. This is mainly due to smaller errors in crossing fibers. This is logical as when two orthogonal compartments are averaged, the best single compartment representing them is almost spherical, meaning a low  $\kappa$  value. The Euclidean distance map in the DWI signal confirms this idea.

### 3.2 MCM Extrapolation on Real Data

The second experiment was to test the entire MCM interpolation pipeline including spectral clustering and free water compartment averaging. We tested methods on a set of 20 real DDI images estimated from DWI with  $128 \times 128 \times 55$  voxels with a  $2 \times 2 \times 2\text{mm}^3$  resolution, 30 gradient directions with one b-value =  $1000 \text{ s.mm}^{-2}$ . In order to assess the quality of interpolation, we extrapolate voxels from their neighborhood. To do so, one in every two voxels are removed and extrapolated from the known remaining values. Input DDI models have three compartments, and so will the extrapolated DDI. Again we compute the Euclidean distance between extrapolated DDI and the original one on the DWI corresponding images. Means are respectively simple: 100, tensor: 84.6, log VMF: 107.0, covariance analytic: 66.2. These results show that covariance analytic performs significantly better than all other methods (paired t-test,  $p < 1.0 \times 10^{-5}$ ) also when used in the complete MCM interpolation framework on real data.

### 3.3 DDI Atlas Construction

The ultimate step of registration of MCM images is the production of an average atlas of the white matter microstructure. We computed an atlas from the 20 DDI images following Guimond et al. atlas construction method [7]. This atlas

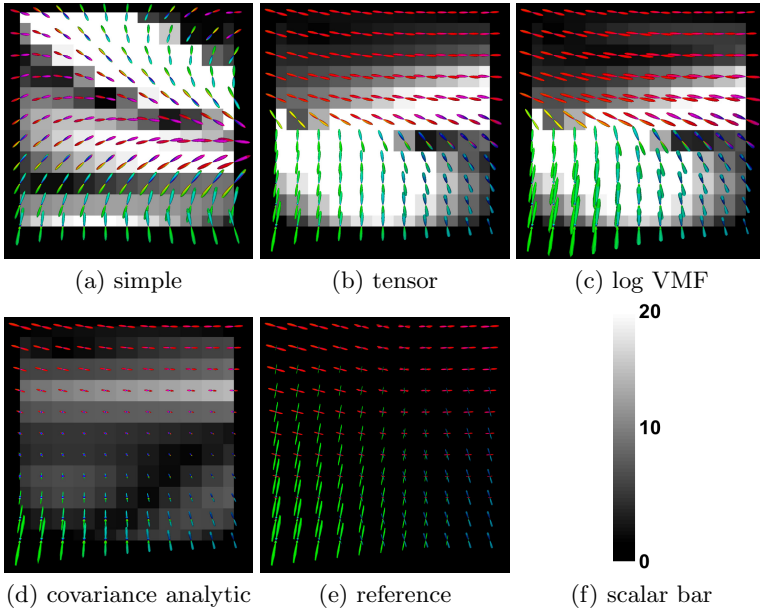


**Fig. 1.** First four images (a-d) illustrate DDI averaging using the four methods superimposed on their local error maps. Image (d) is the reference.

construction was performed using non linear DTI registration as proposed by Suarez et al. [12]. Then, the obtained transformations were applied to the DDI models. We interpolated the DDI models using our clustering approach with the covariance analytic averaging. In addition, when applying a transformation to oriented models, it is necessary to apply the local linear part of the transformation to the interpolated models. We used a technique similar to finite-strain reorientation for tensors [10] by applying the local rotation to the  $\mu_i$  directions of each compartment of the interpolated DDI. We present the visual result of the atlas and a zoomed area in Fig. 2. This atlas provides a clear distinction of crossing fibers and will be of great interest in future studies for example of white matter microstructure destruction in diseases.

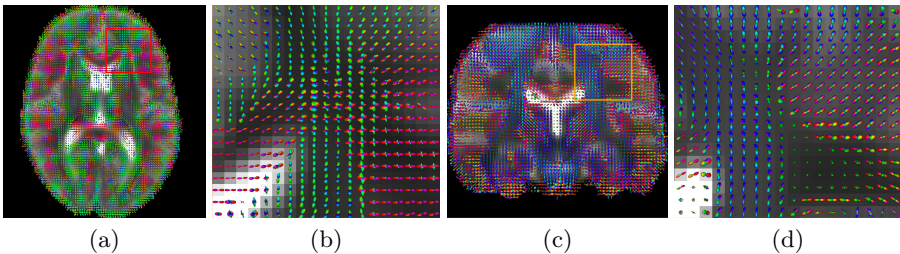


**Fig. 2.** Example of a DDI atlas superimposed on the average B0 image.

## 4 Conclusion

We have addressed the problem of interpolation and averaging of MCM images. As MCMs become increasingly popular and used, the issue of interpolation (e.g. for a registration purpose) or averaging (e.g. for atlas creation) becomes acute in the absence of relevant dedicated solutions yet. We have proposed to perform interpolation as a MCM simplification problem, relying on spectral clustering and compartment averaging methods handling both free water and compartment parameters. For this latter part, we have proposed and compared four different alternatives, these methods being evaluated with synthetic and real data. According to these different experimental conditions, the covariance analytic solution exhibits significantly better performance than the others. This can be explained by its capability to better handle the diffusion dispersion parameter ( $\kappa$ ) around each compartment principal orientation. Although this study has been validated on one MCM model (DDI), the method proposed is generic and may be extended to all currently available MCMs.

## References

1. Arsigny, V., Fillard, P., Pennec, X., Ayache, N.: Log-Euclidean metrics for fast and simple calculus on diffusion tensors. *MRM* 56(2), 411–421 (2006)
2. Barmpoutis, A., Vemuri, B.C., Forder, J.R.: Registration of high angular resolution diffusion MRI images using 4th order tensors. In: Ayache, N., Ourselin, S., Maeder, A. (eds.) *MICCAI 2007, Part I. LNCS*, vol. 4791, pp. 908–915. Springer, Heidelberg (2007)
3. Basser, P.J., Pierpaoli, C.: Microstructural and physiological features of tissues elucidated by quantitative diffusion-tensor MRI. *Journal of Magnetic Resonance, Series B* 111(3), 209–219 (1996)
4. Ferizi, U., Schneider, T., et al.: A ranking of diffusion MRI compartment models with in vivo human brain data. *MRM* 72(6), 1785–1792 (2014)
5. Geng, X., et al.: Diffusion MRI registration using orientation distribution functions. In: Prince, J.L., Pham, D.L., Myers, K.J. (eds.) *IPMI 2009. LNCS*, vol. 5636, pp. 626–637. Springer, Heidelberg (2009)
6. Goh, A., Lenglet, C., Thompson, P.M., Vidal, R.: A nonparametric Riemannian framework for processing high angular resolution diffusion images and its applications to ODF-based morphometry. *Neuroimage* 56, 1181–1201 (2011)
7. Guimond, A., Meunier, J., Thirion, J.P.: Average brain models: A convergence study. *Computer Vision and Image Understanding* 77(2), 192–210 (2000)
8. McGraw, T., Vemuri, B.: Von mises-fisher mixture model of the diffusion ODF. In: *IEEE ISBI*, pp. 65–68 (2006)
9. Ng, A.Y., Jordan, M.I., Weiss, Y., et al.: On spectral clustering: Analysis and an algorithm. *Advances in Neural Information Processing Systems* 2, 849–856 (2002)
10. Ruiz-Alzola, J., Westin, C.F., et al.: Nonrigid registration of 3D tensor medical data. *Medical Image Analysis* 6(2), 143–161 (2002)
11. Stamm, A., Pérez, P., Barillot, C.: A new multi-fiber model for low angular resolution diffusion mri. In: *ISBI*, pp. 936–939. IEEE (2012)



12. Suarez, R.O., Commowick, O., et al.: Automated delineation of white matter fiber tracts with a multiple region-of-interest approach. *Neuroimage* 59(4), 3690–3700 (2012)
13. Taquet, M., Scherrer, B., Commowick, O., Peters, J., Sahin, M., Macq, B., Warfield, S.K.: Registration and analysis of white matter group differences with a multi-fiber model. In: Ayache, N., Delingette, H., Golland, P., Mori, K. (eds.) *MICCAI 2012, Part III*. LNCS, vol. 7512, pp. 313–320. Springer, Heidelberg (2012)